

Thermo-Mechanical Modeling And Analysis Of High Speed Spindle

VVSH Prasad¹ and Dr.V.Kamala²

¹ Department of Mechanical Engineering, Associate Professor, Institute of Aeronautical Engineering, Hyderabad-500043, India

² Retd. Deputy General Manager, Bharath Heavy Electrical Limited- Corporate R&D Division, Hyderabad, India

Abstract

Prediction of the thermo-mechanical behavior of machine-tool spindles is essential in the reliable operation of high speed machine tools. In particular, the performance of these high speed spindles in the order of 20,000rpm is dependent on their structural and thermal behavior. The main source of heat generation in the spindle is the friction torque and viscous friction in angular contact ball bearings. This paper presents an effort to develop a comprehensive design of high speed spindle that includes viable models for the mechanical and thermal behavior of its major components which include bearings, spindle and housing. Mutual interaction between the thermal and structural behavior of both spindle housing and bearings is characterized through application of cutting forces, tool clamping force, drive torque, coupling pressure through power lock along with thermal load. Components are combined to form a finite element analysis model for the thermo-mechanical analysis of spindle-bearing system. Static and dynamic analysis is carried out with all loads to predict structural deformations and stresses developed for different materials at optimal spindle power cutting conditions. The results indicate that the productivity can be enhanced on various materials by applying the optimal cutting parameters on high-speed CNC machine tool with fail safe operations.

Keywords: modeling, analysis, high speed spindle, thermo-mechanical, cutting conditions

1. Introduction

The spindle is the main mechanical component in machining centers/turning centers. The static and dynamic stiffness of the spindle directly affect the machining productivity and finish quality of the work pieces. The structural properties of the spindle depend on the dimensions of the shaft, motor, tool holder, bearings, and the design configuration of the overall spindle assembly [Yao and Hong 2008]. The

bearing arrangements are determined by the cutting operation type, and the required cutting force and life of bearings. The main aim of machine tool design is to achieve long-term precision and high cutting productivity, which directly influence the operating costs of the machine. In high speed machine spindle assembly's bearings plays a major role when it comes to high speeds. A bearing is a machine element that constrains relative motion to only the desired motion, and reduces friction between moving parts. Generally high precision angular contact ball bearings are used in spindle assemblies as they can take both axial loads and radial loads. Hence a study is made in this paper on the behavior of these angular contact ball bearings at different speeds and also its effects on the spindle and machining.

Currently, none of the theoretical analysis can predict the temperature distribution and resulting thermal error of high speed motor spindles with sufficient accuracy. It is necessary to search for accurate functions and procedures to describe the energy losses, the geometry, the heat exchange as well as the dynamics [Yao and Xie 2008]. Normally alloy steel material of grade IS 1570-60 i.e., 21Cr1Mo28(EN36C) is used for manufacturing of high speed hallow spindle with controlled heat treatment process for imparting mechanical properties like case hardness up to 60HRC to a depth of 0.7 to 1.0 mm with tough core for withstanding shock loads for reliable operation to ensure structural stability. A high speed spindle that will be used in a metal cutting machine tool must be designed to provide the required performance features. The major performance features include,

- i. Desired Spindle Power.
- ii. Maximum Spindle Load - Axial and Radial
- iii. Maximum Spindle Speed Allowed
- iv. Tooling Style, Size and Capacity for ATC (Automatic Tool Changing)
- v. Timer Belt Driven Spindle Design
- vi. High running geometrical accuracy
- vii. Great stiffness
- viii. Low and even temperature distribution

ix. Minimum need of maintenance

The following CNC Vertical machining centre is chosen for study and experimentation.

Machine model : AMS spark- Vertical Machining Centre

- Make : ACE Micromatic group
- Spindle taper : 7/24 No. 30
- Spindle speed : 60-6000 rpm
- Spindle speed (opt): 80-8000 rpm
- Spindle power (as shown in fig. 1 and 2) : 5.5/3.75 kW
- Rapid traverse X/Y/Z: 20/20/15 m/min
- Maximum tool weight: 2.5kgf.

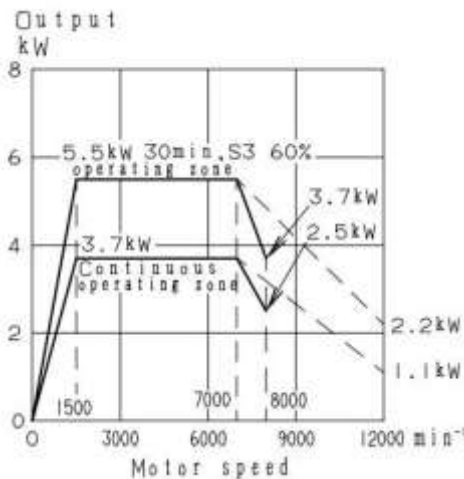


Fig. 1: Motor speed vs power output

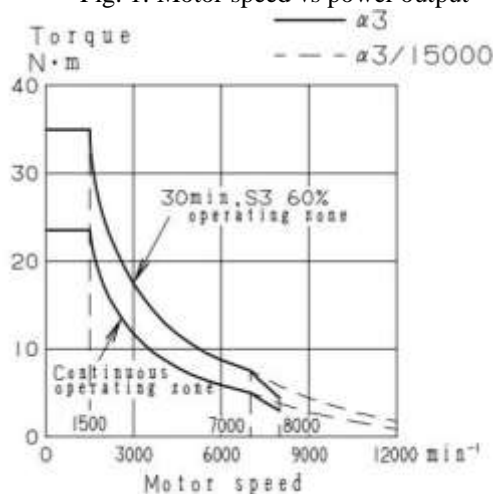


Fig. 2: Motor speed vs torque

1.1 Practical Machining Data

In general CNC machine tools are used for machining of wide variety of materials like soft and hard with infinitely variable spindle speeds and feed rates to optimize cutting parameters and tool life [Chen and Hsu 2003]. In this paper experimentation is carried out on the following materials using standard parameters as shown in the Table 1.

Table 1: Machining data

SI No.	Machining parameter	Units	Steel	Aluminium
1	Brinell hardness	HB	160	50
2	Ultimate tensile strength	N/mm ²	567	200
3	Effective diameter of the cutter	mm	80	40
4	Number of inserts/edges in the cutter	-	6	6
5	Cutting speed v_c	m/min	475	700
6	Axial depth of cut	mm	2	3.5
7	Radial width of cut(75% of the cutter)	mm	60	30
8	Radial engagement factor	-	1	1
9	Machine efficiency factor	-	0.85	0.85

1.2. Cutting Force and Spindle Power

The cutting forces and the spindle power required are shown in Table 2.

Table 2: Cutting force and spindle power for steel and Aluminum

SI No.	Machining parameter	Units	Steel	Aluminum
1	Spindle speed	rpm	1890	5570.4
2	Axis cutting feed rate	mm/min	1701	4456.32
3	Material removal rate	cm ³ /min	204.12	4679.12
4	Tangential force	N	408.2	200.2
5	Torque at the tool tip	N-m	16.33	4.0
6	Power at the cutter	KW	3.2	3.71
7	Power at the motor	KW	3.76	4.36

2. Modeling and Assembly of High Speed Spindle

The designing of high speed spindle carried out in “Solidworks” which is parametric CAD software that helps to create 2D and 3D models in an effective manner.

Drafted view of Spindle assembly (fig. 3) and the bill of materials is given in Table 3, using standard fag bearing specifications, standard disc springs and ISO tool holder.

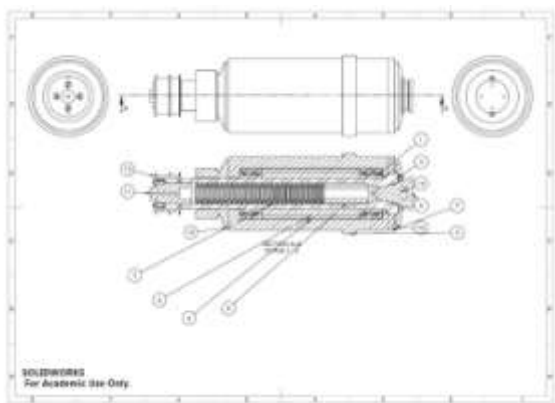


Fig. 3: Assembly of head stock

Table 3: Bill of materials:

S.No	Description	Quantity
1	Angular Contact Ball Bearing (B7009E.P4.UL)	4
2	Spacer Cyl.Inner	1
3	Spindle	1
4	Spacercyl.Outer	1
5	Spindle Housing-Cartridge	1
6	Rod Draw Bar	1
7	Disc Spring-Size 31.5x16.3x1.75mm	88
8	Spacercyl.Outer	1
9	Cover End	
10	Flange Cover	1
11	Bush Guide (Bt30)	1
12	Flange Cover-Rear	1
13	H.S.H.C Screw M6x25	6
14	Tool Holder (BT30)	1

Section view of the spindle assembly is shown in fig. 4 detailing bearing pre load and tool bar clamping force.

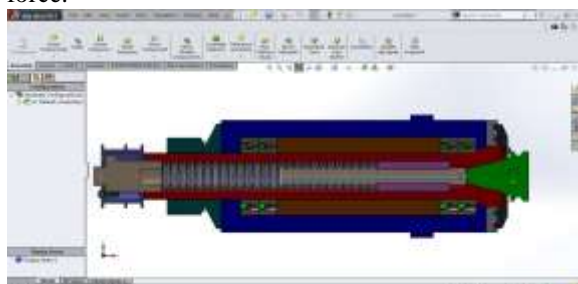


Fig. 4: Section view of the head stock assembly

Exploded view of spindle assembly is shown in fig. 5.



Fig. 5: Exploded view of spindle assembly

2.1 Thermal modeling

The mechanical and thermal processes in a bearing are coupled. This coupling manifests itself in the thermal expansion of components and the change of mechanical properties due to heat flow through mechanical parts [Lin a, Jay F Kamman 2003 and Arakere, Schmitz, Cheg,]. The temperature at which a bearing operates depends on factors, such as applied load, operating speeds, lubricant properties, bearing arrangement, and housing design and environment. All these factors affect either heat generation or heat transfer. The thermal model includes heat generation and heat transfer within the bearing and the spindle shaft and housing.

Heat generation

Heat generation in angular contact ball bearings can be load-related, viscosity-related and/or spin-related.

- **Load related heat generation**

The friction torque, M_l , leading to load-related heat generation, can be calculated:

$$M_l = f_1 F \beta d_m$$

Where, d_m is the mean diameter of the bearing. If F_a and F_r are bearing axial and radial loads, respectively, and θ is the nominal contact angle (the contact angle at no-load condition), $F\beta$ is obtained as below

$$F\beta = \max(0.9F_a \cot \theta - 0.1F_r, F_r)$$

$$d_m = 60 \text{ mm}$$

$$\text{Axial force, } F_a = f_z i z D^2 \cos \alpha = 5.59 \text{ KN}$$

$$\text{Radial force } F_r = f_z z D^2 \sin \alpha = 12.8 \text{ KN,}$$

$$\text{where } i=1, z=21, D=5 \text{ mm, } \alpha=30^\circ, f_z=12.3.$$

$$\text{therefore, } F\beta = \max(7.43, 12.8) = 12.8 \text{ KN}$$

$$f_1 = Z(F_s / F_a)^y = 1.136 \times 10^{-3}$$

$$\text{where } F_s = X F_r + Y F_a = 8.24 \text{ KN}$$

$$\text{Now, } M_l = 0.8724 \text{ W}$$

- **Viscosity related**

$$M_v = f_0 (v_0 N)^{2/3} d_m \times 10^{-7} = 16.92 \text{ W}$$

$$\text{Where } v_0=0.67, N=6000 \text{ rpm.}$$

- **Spin related**

$$M_s = 35.43 \times 10^{-3} \text{ W}$$

Where μ is friction factor, a is the major axis of the elliptical contact zone, E is the elliptical integral of a 2nd kind over the contact area and F is preload.

$$\mu = 0.01, a=45 \text{ mm, } E=0.7, F=300 \text{ N}$$

2.2 Bearing Model

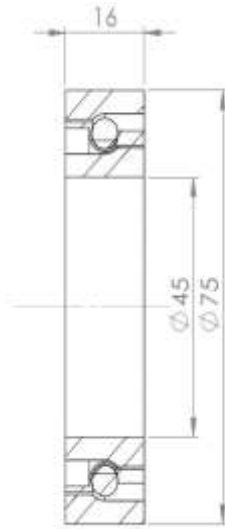


Fig. 6: Angular contact ball bearing

The specifications of the bearing shown in fig. 6 are as follows:

Bearing code – B7009EP4U

Inner diameter – 45 mm

Outer diameter – 75 mm

Width – 16 mm

Dynamic load – 26.5 kN

Static load rating – 20.0 kN

Mass – 0.23 kg

Limiting speed with grease lubrication – 17000 rpm

Limiting speed with oil lubrication – 28000 rpm

3. Analysis of Spindle

The analysis was carried out in ANSYS Workbench. Table 4 indicated constitutive relations of the spindle material.

Table 4: Properties of 21Cr1M028 (EN36C) case carburizing steel [Choi and Lee 1998]

Density	7.87 g/cm ³
Hardness, Brinell	341 HB
Ultimate Tensile Strength (UTS)	1100 MPa
Yield Strength (YS)	770 MPa
Modulus of Elasticity	209 GPa
Poissons Ratio	0.29
Shear Modulus	80 GPa

As per the ASTM standards, the following standards have been considered for induced stress in the spindle material [Chen and Cgen 2005]. It is considered as 18 % of the UTS or 30 % of the YS whichever is low for considering the failure criteria. If the spindle is having keyway, the values are considered 75 % of the ASTM standards.

It is given as,

$$0.18 \times 1100 \times 0.75 = 148.5 \text{ MPa}$$

$$0.3 \times 770 \times 0.75 = 173.25 \text{ MPa}$$

Table indicates the loads applied for static and dynamic analysis.

Table 5: Loads applied for static and dynamic analysis

Tangential cutting force	684 N
Tool clamping force	3.75 kN
Torque applied at motor side	23.5 N-m
Clamping pressure applied by power-lock	225 MPa
Thermal load	51.56 W

The 3D model of spindle is shown in fig. 7, and the meshing done is shown in fig. 8.

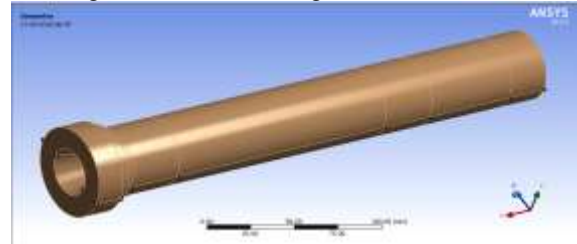


Fig. 7: 3D model of spindle

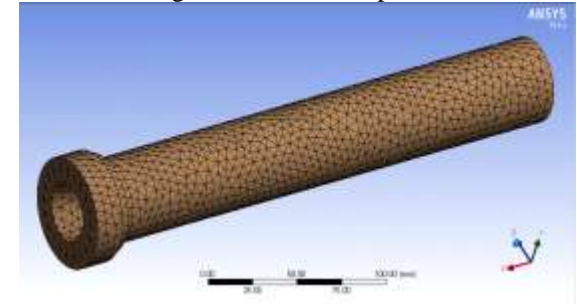


Fig. 8: Spindle meshed to required specification (TET10)

3.1 Steady State Thermal Analysis

Steady state thermal analysis has been carried out by applying thermal load of 51.56 W at 6000 rpm as shown in fig. 9.

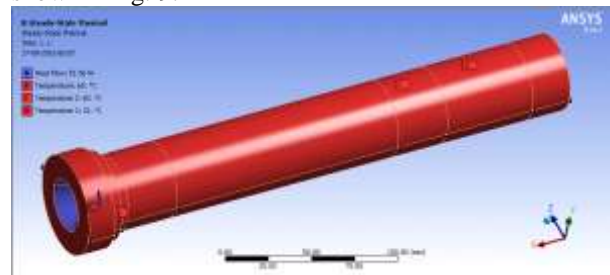


Fig. 9: Steady state thermal analysis done on the spindle

It is observed that bearing zone is getting heated up to 60 °C and remaining area found to be at 35 °C, fig. 10, and thermal heat flux is shown in fig. 11, along the tool bearing area. However, during metal cutting using emulsion cutting fluid at 20 °C will bring down the bearing zone temperature by conduction heat transfer at cutting zone.

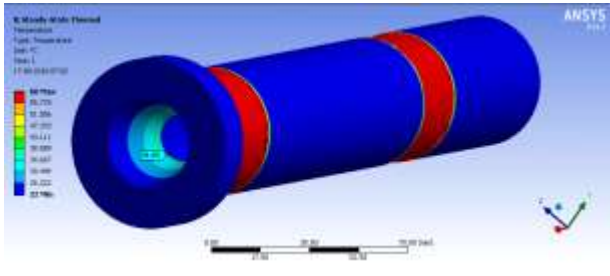


Fig. 10: Temperature gradient

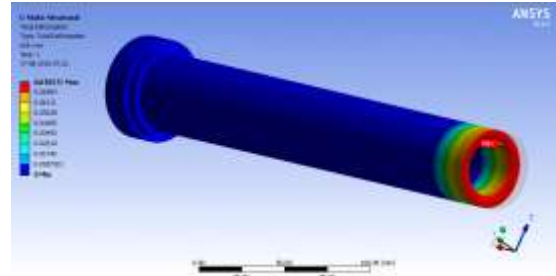


Fig. 13: Total deformation

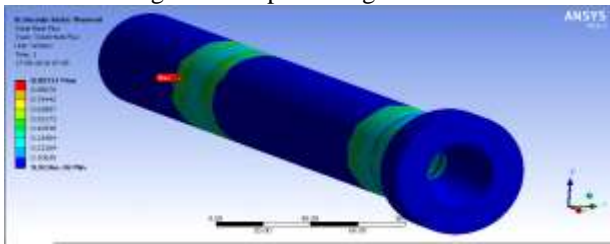


Fig. 11: Thermal heat flux

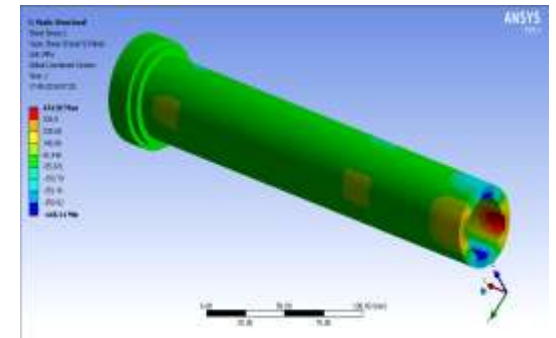


Fig. 14: Shear stress in YZ plane

3.2 Static Structural Analysis (Case – 1)

Static structural analysis both front and rear bearing constraint was done. Applying the loads (as given in table), along with thermal load, it was found that the deformation at BT-30 tool taper face $0.004 \mu\text{-m}$ and at power-lock coupling face $0.078 \mu\text{-m}$ with induced stress of 920 MPa. However, this deviation shall be nullified as the stress flow takes place in the rear cover and spindle house. The Vonmises stress analysis is shown in fig. 12. The total deformation is shown in fig. 13. The shear stress in YZ plane is shown in fig. 14. The reactions at bearing near tool holder is shown in fig. 15. The reactions at bearing near power-lock is shown in fig. 16.

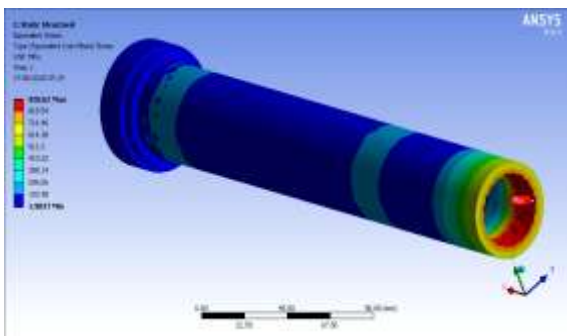


Fig. 12: Vonmises stress analysis

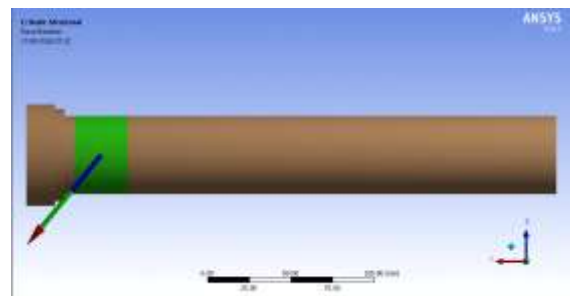


Fig. 15: Reactions at bearing near tool holder

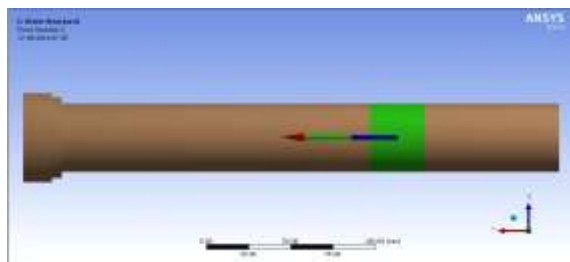


Fig. 16: Reactions at bearing near power-lock

3.3 Static Structural Analysis (Case – 2)

Static structural analysis with front bearing applied cylindrical support was done. Applying the loads (as given in table), and varying the front bearing as cylindrical support, the rear bearing reaction found to be 3.138 kN @ 270° which is less than the static and dynamic stiffness of the bearings. Other observations remain same. Hence design is safe. The front cylindrical support boundary condition is shown in fig. 17. The Vonmises stress analysis is shown in fig. 18. The total deformation is shown in fig. 19. The shear stress in YZ plane is shown in fig. 20. The

reactions at bearing near power-lock is shown in fig. 21.

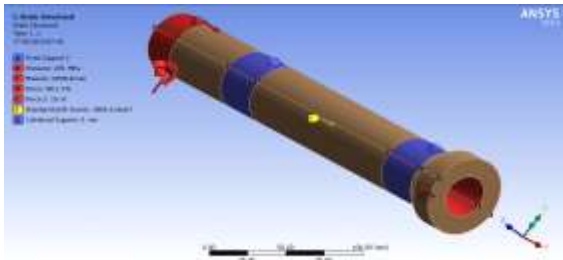


Fig. 17: Front cylindrical support boundary condition

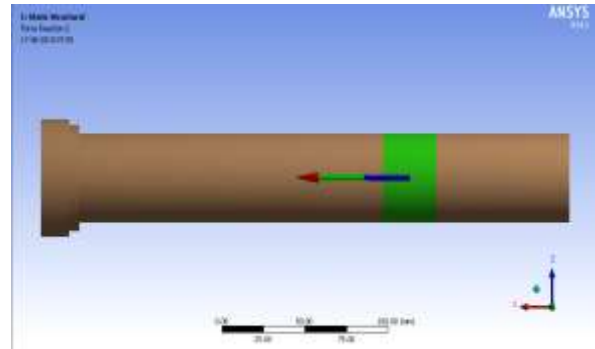


Fig. 21: Reactions at bearing near power-lock

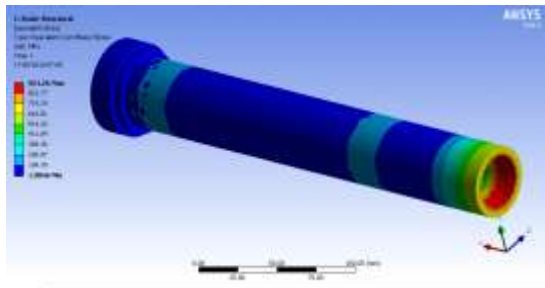


Fig. 18: Vonmises stress analysis

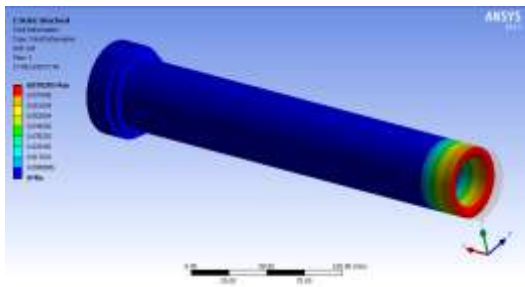


Fig. 19: Total deformation

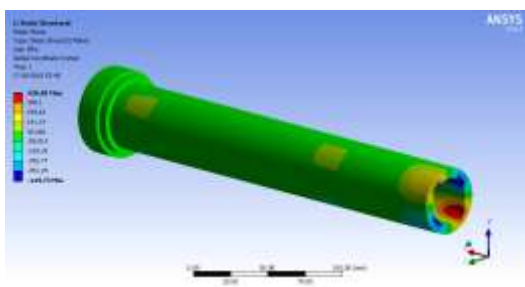


Fig. 20: Shear stress in YZ plane

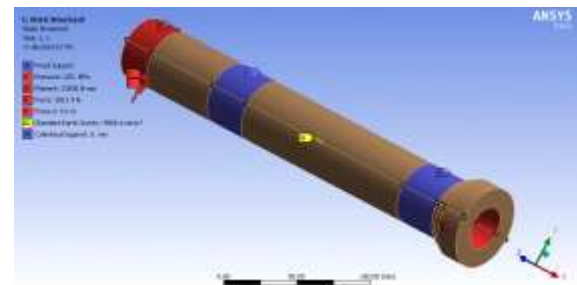


Fig. 22: Front cylindrical support boundary condition

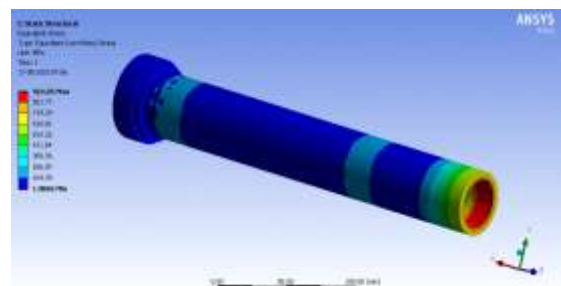


Fig. 23: Vonmises stress analysis

3.4 Static Structural Analysis (Case – 3)

Static structural analysis with rear bearing applied cylindrical support was done. Applying the loads (as given in table), and varying the rear bearing as cylindrical support, the front bearing reaction found to be 1.3 kN @ 225° which is less than the static and dynamic stiffness of the bearings. Other observations remain same. Hence design is safe. The rear cylindrical support boundary condition is shown in fig. 22. The Vonmises stress analysis is shown in fig. 23. The total deformation is shown in fig. 24. The shear stress in YZ plane is shown in fig. 25. The reactions at bearing near tool holder are shown in fig. 26.

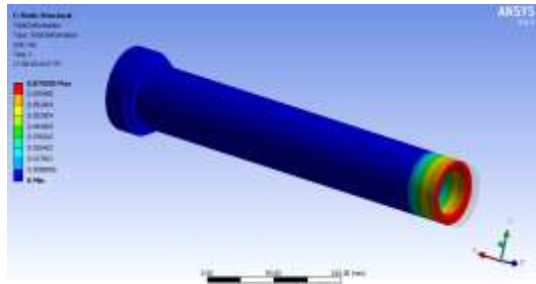


Fig. 24: Total deformation

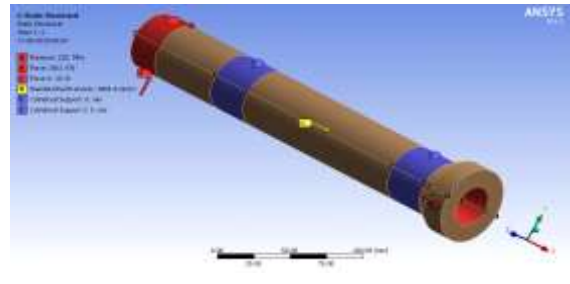


Fig. 27: Rear cylindrical support boundary condition

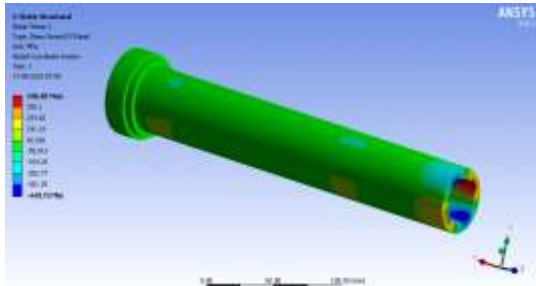


Fig. 25: Shear stress in YZ plane

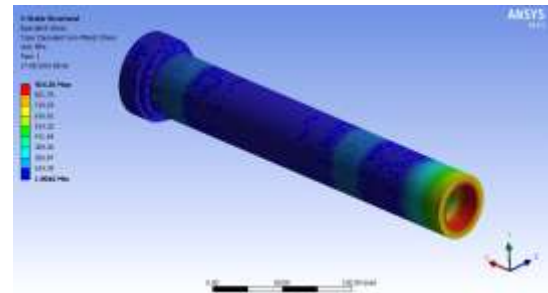


Fig. 28: Vonmises stress analysis

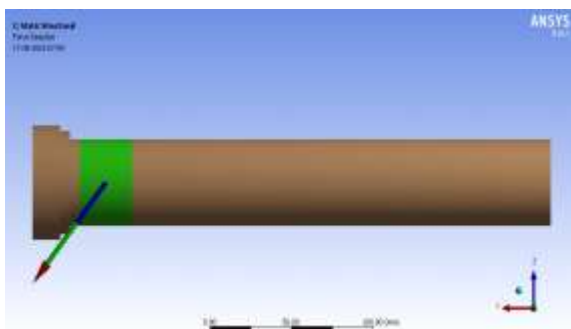


Fig. 26: Reactions at bearing near tool holder

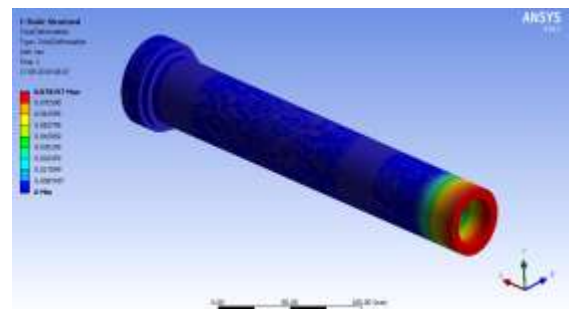


Fig. 29: Total deformation

3.5 Static Structural Analysis (Case – 4)

Static structural analysis with front and rear bearing applied cylindrical support was done. Applying the loads (as given in table), and varying the front and rear bearing as cylindrical supports, the front bearing reaction found to be 1.3 kN @ 225° and rear bearing reaction found to be 3.138 kN @ 270°. The induced stresses are fail safe and deformations with the given limits. The rear cylindrical support boundary condition is shown in fig. 27. The Vonmises stress analysis is shown in fig. 28. The total deformation is shown in fig. 29. The shear stress in YZ plane is shown in fig. 30.

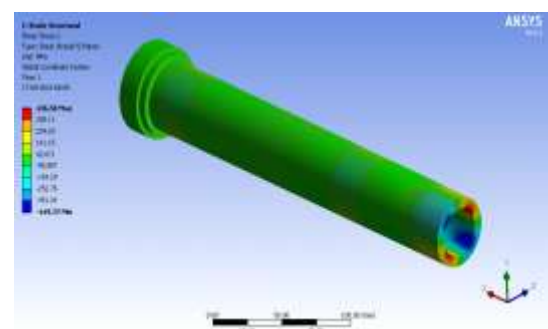


Fig. 30: Shear stress at YZ plane

4. Results and Discussion

The coupling pressure is predominant at the rear bearing side showing deformation and induced stresses. These stresses will flow in the rear flange, spindle and bearing housing, and on to the timer pulley. The induced stresses are below 148 MPa in

the assembly analysis with mutual interaction of the assembly components.

When the spindle is delivering 3.7 kW power during face milling operations, the stress induced is below the allowable stress of 143.5 MPa. Hence, the design is safe.

The summary of results obtained is given in the table 6.

Table 6: Summary of results

ANALYSIS	CASE – I	CASE – II	CASE – III	CASE – IV	CONCLUSION
Vonmises-@power lock	924 MPa	924 MPa	924 MPa	924 MPa	Shall be concluded in assembly analysis
Vonmises-@ bearing faces	143 MPa	143 MPa	143 MPa	143 MPa	Safe
Total deformation @ power lock	0.079 mm	0.079 mm	0.079 mm	0.079 mm	Shall be concluded in assembly analysis
Total deformation @ tool holder face	0.004 mm	0.004 mm	0.004 mm	0.004 mm	Safe
Reaction at bearing @power lock	1963 N @ ~ 270 DEG	3138 .6 N @ ~ 270 DEG	NA	NA	Safe
Reaction at bearing @ tool holder	901.7 N @ ~ 225 DEG	NA	902.51 N @ ~ 225 DEG	NA	Safe

5. Conclusions

1. The power requirement for machining of Steel is 3.2 kW at the tool tip and rated output of spindle motor is 3.75 kW. About 85 % operational efficiency is achieved.
2. The power requirement for machining of Aluminum is 3.71 kW at the tool tip and rated output of spindle motor is 3.75 kW. About 98.93 % operational efficiency is achieved. However, if mechanical efficiency transmission losses are also considered then spindle motor can deliver 5

kW output in 30 minutes rating. This clearly shows that optimum utilization of spindle power for increasing the productivity in the assembly lines.

3. The torque requirement for machining of steel is 16.33 N-m which is below rated torque of 23.5 N of the servo motor with a base speed of 1500 rpm.
4. The material removal rate in case of Aluminum is considerably high i.e., 4679.115 cc/min.
5. The tool life optimization will be achieved by using suitable cutting speeds which reduces the tooling cost. The tool replacement strategies can be planned for augmentation of the tool inventories.
6. From the analysis results it was observed that the bearing reactions of 1.3 kN at front and 3.138 kN at the rear are well within the static and dynamic load rating of the bearings.
7. Thermal load is not having impact on the spindle performance.

Acknowledgments

The authors would like to thank the Principal of Institute of Aeronautical Engineering for his encouragement, support and granting permission to publish this work. The authors also express their sincere thanks to the authorities of Osmania University, Hyderabad for their support and permission to present this work.

References

- [1] Chi-Wei Lin a, Jay F. Tua, Joe Kamman, “An integrated thermo-mechanical-dynamic model to characterize motorized machine tool spindles during very high speed rotation”, International Journal of Machine Tools & Manufacture 43 1035–1050(2003)
- [2] Jenq-Shyong Chen Wei-Yao Hsu, “Characterizations and models for the thermal growth of a motorized high speed spindle” International Journal of Machine Tools & Manufacture 43 1163–1170(2003)
- [3] Jin Kyung Choi, Dai Gil Lee, “Thermal characteristics of the spindle bearing system with a gear located on the bearing span”, Department of Mechanical Engineering,

- Korea Advanced Institute of Science and Technology, ME3221-1998.
- [4] Jenq-Shyong Chen, Kwan-Wen Chen, “Bearing load analysis and control of a motorized high speed spindle”, International Journal of Machine Tools & Manufacture 45 1487–1493(2005)
- [5] Nagaraj Arakere, Tony L. Schmitz, Chi-Hung Cheng, “Rotor Dynamic Response of a High-Speed Machine Tool Spindle”, University of Florida, Department of Mechanical and Aerospace Engineering 237 MAE-B, Gainesville, FL 32611 .
- [6] Y. Lu Y.X. Yao and R.H. Hong, “Finite Element Analysis of Thermal Characteristics of High-speed Motorized Spindle”, Applied Mechanics and Materials Vols. 10-12 pp 258-262 (2008)
- [7] Y. Lu Y.X. Yao and W.Z. Xie, “Finite Element Analysis of Dynamic Characteristics of High-speed Motorized Spindle”, Applied Mechanics and Materials Vols. 10-12 pp 900-904 (2008)